Conf-940395--1

UCRL-JC-116505
PREPRINT

# Issues in the Design and Optimization of Adaptive Optics and Laser Guide Stars for the Keck Telescopes

C.E. Max, D.T. Gavel, S.S. Olivier, J.M. Brase,
H.W. Friedman, K. Avicola, J.T. Salmon,
A.D. Gleckler, T.S. Mast, J.E. Nelson, P.L. Wizinowich
G.A. Chanan

This paper was prepared for submittal to the
*Astronomical Telescopes & Instrumentation*
*for the 21st Century*
*Kona, Hawaii*
*March 13-18, 1994*

March 1994

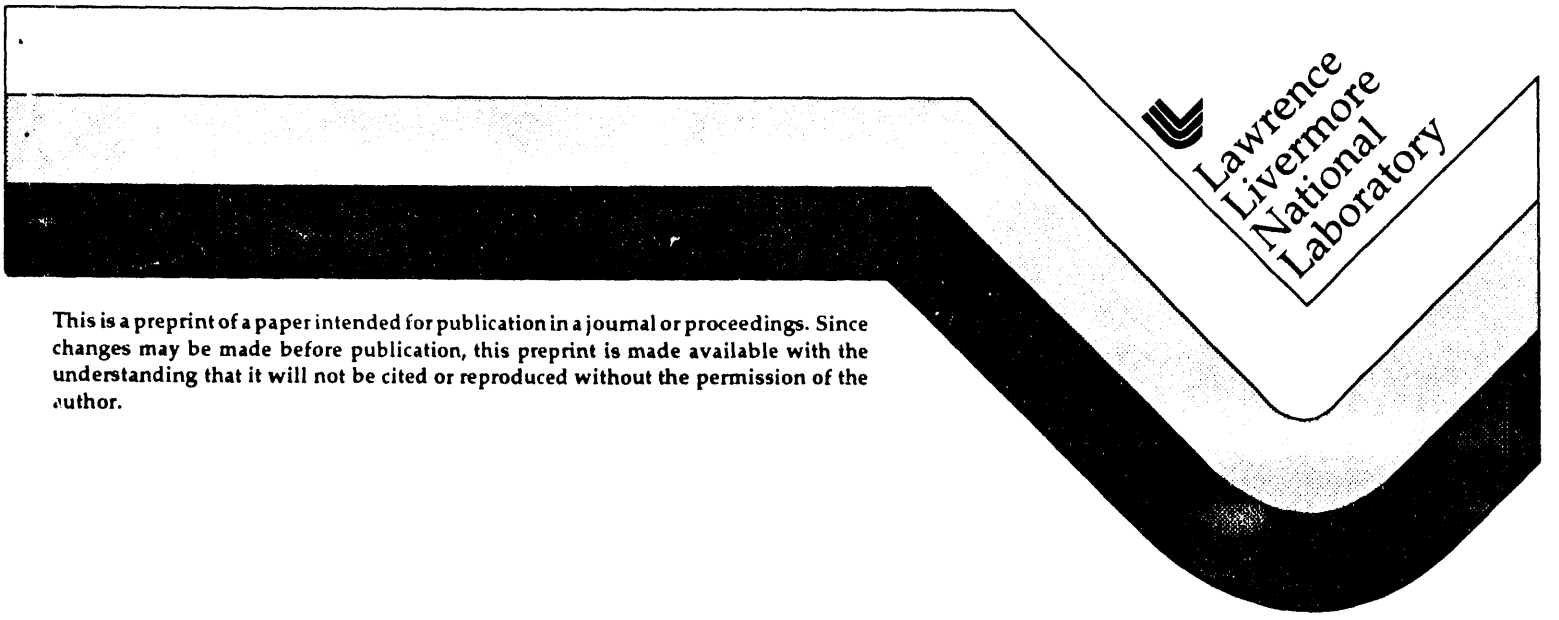

# Issues in the design and optimization of adaptive optics and laser guide stars for the Keck Telescopes

C. E. Max, D. T. Gavel, S. S. Olivier, J. M. Brase, H. W. Friedman, K. Avicola, J. T. Salmon

Lawrence Livermore National Laboratory
P. O. Box 808, Livermore, CA 94550

A. D. Gleckler, T. S. Mast, J. E. Nelson, P. L. Wizinowich

W. M. Keck Observatory
P. O. Box 220, Kamuela HI 96743

G. A. Chanan

Physics Department, University of California
Irvine, CA 92717

## ABSTRACT

We discuss issues in optimizing the design of adaptive optics and laser guide star systems for the Keck Telescope. The initial tip-tilt system will use Keck's chopping secondary mirror. We describe design constraints, choice of detector, and expected performance of this tip-tilt system as well as its sky coverage. The adaptive optics system is being optimized for wavelengths of 1 - 2.2 μm. We are studying adaptive optics concepts which use a wavefront sensor with varying numbers of subapertures, so as to respond to changing turbulence conditions. The goal is to be able to "gang together" groups of deformable mirror subapertures under software control, when conditions call for larger subapertures. We present performance predictions as a function of sky coverage and the number of deformable mirror degrees of freedom. We analyze the predicted brightness of several candidate laser guide star systems, as a function of laser power and pulse format. These predictions are used to examine the resulting Strehl as a function of observing wavelength and laser type. We discuss laser waste heat and thermal management issues, and conclude with an overview of instruments under design to take advantage of the Keck adaptive optics system.

## 1. BRIEF OVERVIEW OF KECK ADAPTIVE OPTICS PROGRAM PLAN

The Keck Adaptive Optics Science Team has developed an implementation plan for adaptive optics[1]. The is a phased plan; each phase will take advantage of lessons learned in previous ones. The plan consists of the following sequence of "Facilities":

- Facility I implements tip-tilt correction using the chopping secondary mirror on the Keck I telescope. It serves the infra-red instruments at the forward Cassegrain focus. On Keck II, tip-tilt correction will use the Infra-Red Fast Steering Mechanism.

- Facility II consists of an infra-red-optimized adaptive optics system, located on one of the Nasmyth platforms.

- Facility III adds laser guide star capability, via a sodium-layer-based artificial beacon system. This phase begins with one laser beacon to increase the sky coverage of the Facility II infra-red adaptive optics system (Facility IIIa). Later, visible adaptive optics will be provided by the installation of multiple laser beacons and an upgraded adaptive optics system (Facility IIIb).

- Facility IV implements interferometry using the two ten-meter Keck telescopes together with smaller outrigger telescopes[2]. Adaptive optics will be used to phase the ten-meter telescope apertures; the outrigger telescopes will use tip-tilt correction.

Details of the Program Plan are discussed in Reference 1. In the present paper we will address issues regarding design optimization for Facilities I, II, and IIIa. We will emphasize optimization of sky coverage and Strehl ratio, for a range of observing wavelengths and a variety of candidate laser systems.

## 2. DESIGN ISSUES FOR TIP-TILT CORRECTION

Tip-tilt correction can improve images by removing the centroid motion due to atmospheric turbulence, and also by removing the effects of mechanical vibration and wind-buffeting of the telescope structure itself.

Centroid motion due to atmospheric turbulence is predicted to yield the most dramatic image improvement when the telescope diameter D is at most 3 - 5 times the atmospheric coherence length $r_0$ (the so-called Fried parameter). Using a value $r_0 = 20$ cm at 0.5 μm wavelength as typical of the Mauna Kea site, and scaling $r_0$ to wavelengths longer than 0.5 μm according to $r_0(\lambda) \propto \lambda^{1.2}$, this would imply that the most benefit from tip-tilt correction would occur at wavelengths longer than 4 - 6 μm, for a ten-meter telescope.

Figure 1 illustrates this effect, plotting the Strehl ratio for tip-tilt correction as a function of observing wavelength, for an assumed Hufnagel-Valley atmospheric turbulence model with coherence length $r_0 = 20$ cm at 0.5 μm, isoplanatic angle $\theta_0 = 20$ μrad, and Greenwood frequency $f_G = 50$ Hz. The solid curve is the long-exposure Strehl ratio expected with no tip-tilt correction. The dashed curve shows the improved Strehl expected if tip-tilt correction could be done perfectly. One sees that at wavelengths shorter than 3 - 4 μm, tip-tilt correction alone is insufficient to provide a high Strehl ratio for a ten meter telescope.

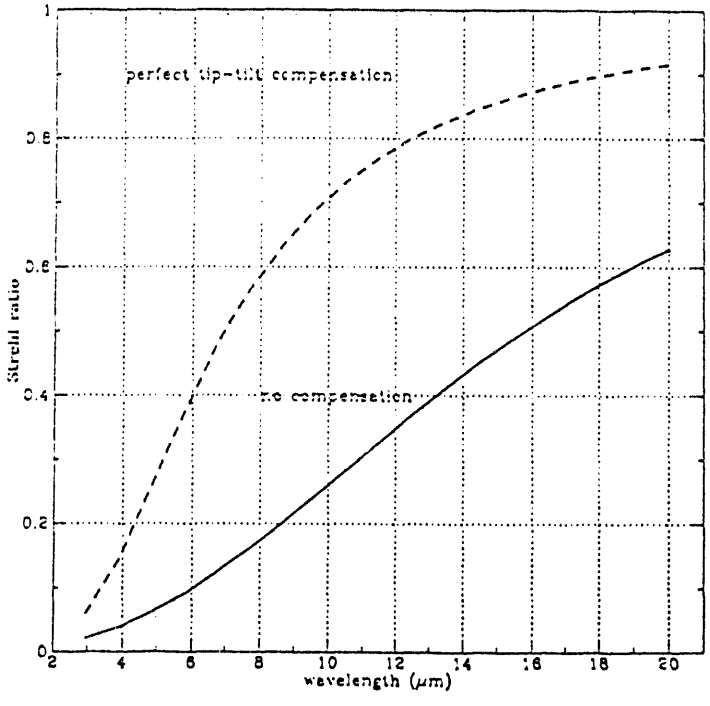


Figure 1. Strehl ratio expected for no compensation (solid curve) and perfect tip-tilt correction (dashed curve), as a function of observing wavelength. A Hufnagel-Valley atmospheric turbulence model was assumed, with Fried coherence length $r_0 = 20$ cm at 0.5 μm, isoplanatic angle $\theta_0 = 20$ μrad, and Greenwood frequency $f_G = 50$ Hz.

Tip-tilt correction will also compensate for mechanical vibration and wind-buffeting. The latter two corrections are, of course, independent of observing wavelength, and have no isoplanatic angle associated with them. Thus the actual image improvement seen with a tip-tilt system may be considerably larger than the ratio of the dashed and solid curves in Figure 1, if mechanically induced centroid motions are comparable to or larger than those induced by atmospheric turbulence. On a summit such as Mauna Kea with relatively high median wind speeds, the benefits of mechanical image stabilization can be substantial. Dekens et al.[3] are in the midst of a program to characterize both the mechanical and atmospherically induced components of centroid motions on the Keck I telescope.

The dotted curve shown in Figure 1 makes the idealized assumption that tip-tilt has been perfectly corrected. Of course in reality the tip-tilt correction will have some residual wavefront error. This is due to several effects: finite control loop bandwidth, finite signal to noise ratio of the sensor, and finite tilt isoplanatism (because there will usually not be a tip-tilt reference star near the center of the field of view). To these error terms must be added another, centroid anisoplanatism[4]. The physical origin of centroid anisoplanatism is as follows. If the tip-tilt sensor performs a centroid measurement, the centroid position is not a fully accurate indicator of the Zernike tilt, because there are atmospherically induced coma aberrations which are asymmetric, and thus can "fool" the centroid determination.

In the face of these wavefront error terms one can nevertheless optimize the tip-tilt correction[5,6], given the statistical distribution of tip-tilt reference stars on the sky (including both their magnitudes and positions). The optimization process trades off the various terms in the error budget, to arrive at the best wavefront correction for a given magnitude of reference star. For example, if one samples the reference star at a lower bandwidth, one can collect more photons (higher signal to noise ratio) at the cost of a larger control loop phase lag. Similarly, because there are fewer bright stars than dim stars in the sky, one can trade off tilt anisoplanatism errors with signal-to-noise errors by using a dimmer reference star that is closer by in angle on the sky.

Figure 2 illustrates the RMS wavefront error resulting after this optimization, as a function of the statistical sky coverage fraction over which each correction will be achievable. A Mauna Kea atmosphere is assumed, as above. The curves shown are as follows (bottom to top): $\sigma_{bw}$ is the error due to finite bandwidth effects, $\sigma_{snr}$ is the error due to finite signal to noise, $\sigma_{ta}$ is the error due to tilt anisoplanatism, $\sigma_{tilt\text{-}ca}$ is the sum of all the previous errors, and represents the total tilt error *minus* that due to centroid anisoplanatism, $\sigma_{ca}$. The top curve, $\sigma_{tilt}$, is the total tilt wavefront error if a centroiding algorithm is being used.

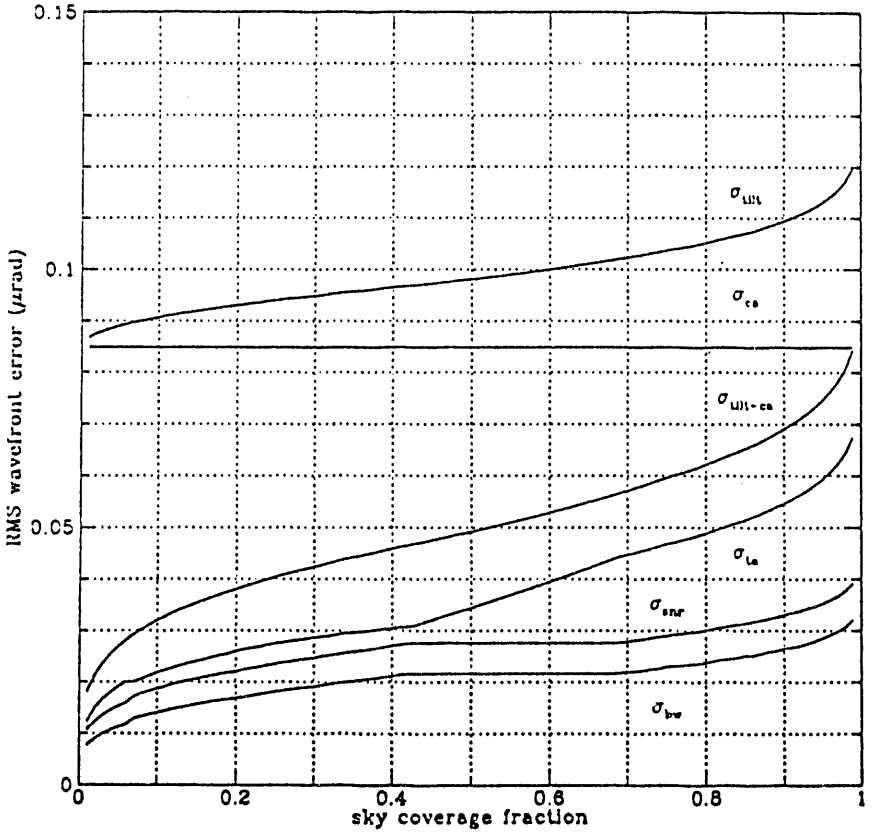


**Figure 2 . RMS residual wavefront error for tip-tilt correction after statistical optimization, for a 10 meter telescope on Mauna Kea. The top curve, $\sigma_{tilt}$, represents the total residual tilt with use of a centroiding detector. The second curve, $\sigma_{ca}$, represents centroid anisoplanatism. The third curve from the top, $\sigma_{tilt\text{-}ca}$, represents the tip-tilt correction attainable if a sensor is used which can remove coma terms, thus measuring the Zernike tilt.**

The reader should note the large difference between the top curve, $\sigma_{tilt}$, and the third curve, $\sigma_{tilt\text{-}ca}$. At Mauna Kea with an 8 or 10 meter telescope, one can improve the residual wavefront error by about a factor of two over 50% of the sky, if one uses a tip-tilt sensor which can measure the Zernike tilt rather than doing centroiding. As a consequence of these considerations, the tip-tilt sensor which has been chosen for the Keck system is a $64^2$ low-noise CCD camera, which can be used in a wavefront sensor mode to subtract out the offending coma aberrations and measure a good approximation to the Zernike tilt. In that case the tilt removal should have a residual wavefront error of about 0.05 μrad or 0.01 arc sec over 50% of the sky.

Because all but the dimmest stars are separated by relatively large distances on the sky, to achieve good sky coverage in Figure 2 one must use tip-tilt reference stars which are quite faint. In this case the optimization process leads one to use low control-loop bandwidths, in order to collect more photons from the (dim) reference star.

Figure 3 shows the optimum tip-tilt reference star magnitude $m_V$ as well as the optimum closed-loop bandwidth. These are calculated together with the top curve $\sigma_{tilt}$ in Figure 2 as part of the optimization process. In order to achieve 50% sky coverage on a statistical basis, Figure 3 shows that the optimal reference star magnitude for a ten meter telescope is $m_V = 19$, while the optimal closed-loop bandwidth is only 3 Hz.

The latter may seem surprising at first sight, since it is much slower than the Greenwood frequency $f_G = 50$ Hz. Tracking applications in a military context have customarily used far larger bandwidths for their control systems. However, the very large aperture of a ten meter telescope makes the frequencies typical of centroid motion quite slow. In addition, the available guide stars are very dim if one wants to achieve high sky coverage, so one must use a longer integration time to reach acceptable signal to noise ratios. Under these circumstances the error due to the finite 3 Hz bandwidth is relatively small (the finite bandwidth term is in fact the smallest error contributor in Figure 2).

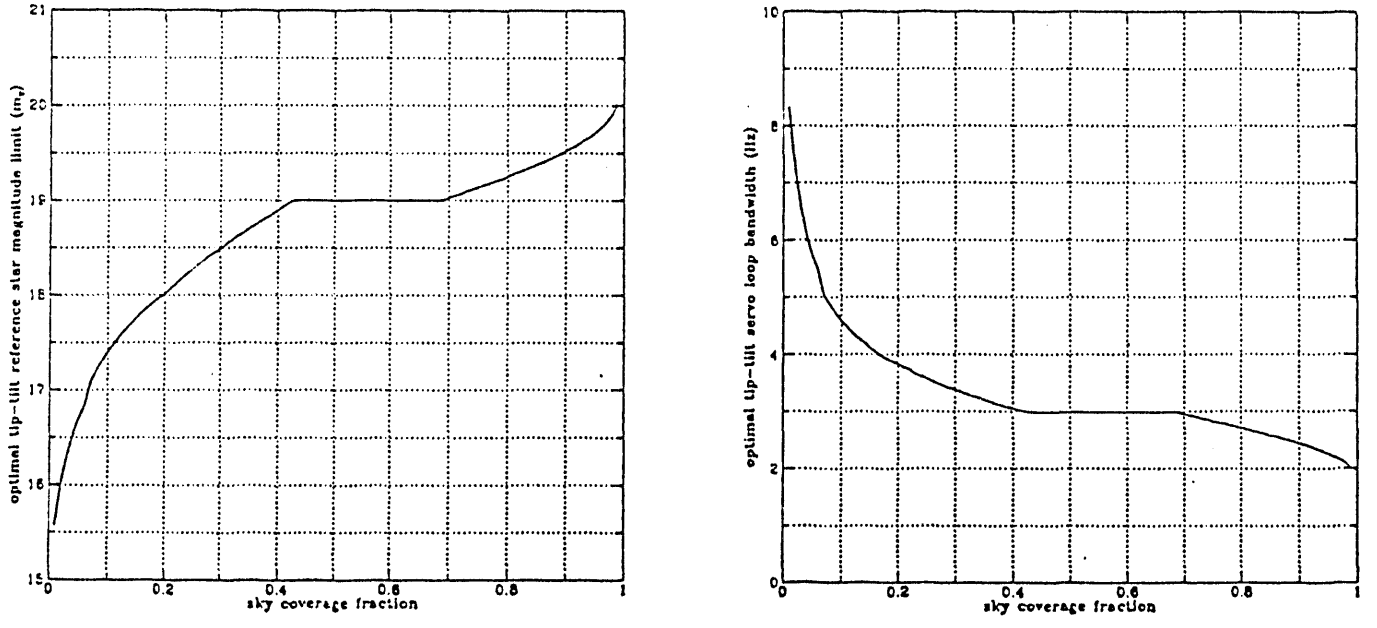


Figure 3. Optimal tip-tilt reference star magnitude $m_V$ and optimal closed-loop bandwidth, as a function of the statistical sky coverage fraction. Calculations are for a ten meter telescope and the same Mauna Kea atmospheric turbulence conditions assumed for Figures 1 and 2. For 50% sky coverage, the optimal tip-tilt reference star magnitude is $m_V = 19$, while the optimal closed-loop bandwidth is 3 Hz.

Of course if an astronomical observer is lucky enough to be interested in an object which is itself inherently bright, or if it has a bright object near by, one will want to retain the ability to run the tip-tilt control loop at a bandwidth much faster than the statistically determined optima shown in Figure 3. Thus it is important to design a tip-tilt system which has the capacity to run at bandwidths of the order of 100 - 200 Hz, in order to take advantage of bright reference objects and run with high winds.

## 3. INFRA-RED ADAPTIVE OPTICS WITH NATURAL GUIDE STARS

### 3.1 Performance optimization using a flexible number of subapertures

One of the dilemmas facing the designer of astronomical adaptive optics is how to optimize a given hardware system for a range of different atmospheric turbulence conditions (e.g. $r_0$ variations from 10 to 30 cm at $\lambda$ = 0.5 μm) and a range of observing wavelengths (e.g. from 1 to 5 μm, the range of typical near-infra-red detectors). The approach we are pursuing is to choose a deformable mirror with as many degrees of freedom as we can afford, but to develop the capability to "gang together" groups of deformable mirror subapertures under software command, to make the system act as if it had larger effective subapertures and fewer degrees of freedom when circumstances demanded.

This would require the wavefront sensor to have a variable number of subapertures, in order to make most effective use of the photons from the reference star or laser star. For example, a Hartmann wavefront sensor could be equipped with a variety of lenslet arrays and their companion optics, which could be changed at the beginning of the night to suit the desired observing wavelength and the local seeing conditions. Alternatively, a shearing interferometer with variable shear could be used. The hardware and software needed to implement this approach has not yet been designed in detail. But the optimization studies which we have done all highlight the potential importance of being able to respond flexibly to the conditions at hand.

By analogy with the optimization of tip-tilt correction described in Section 2 above, one can optimize the performance of a natural guide star adaptive optics system[7] by varying the number of effective subapertures (up to the physical limit of a particular deformable mirror) and varying the control loop bandwidth, as a function of observing wavelength and natural guide star magnitude (or alternatively, sky coverage fraction). Figure 4 shows the results of such optimization, plotting Strehl versus reference star magnitude $m_R$ for various observing wavelengths. The top panel of Figure 4 is for a deformable mirror which can be configured with up to 36 subapertures, the central panel is for a deformable mirror with ≤ 121 effective subapertures, and the bottom panel for a mirror with ≤ 441 effective subapertures. The optimization was allowed to choose the number of effective subapertures used in each case. Turbulence parameters for this calculation are the same as for the previous Figures. CCD read noise and quantum efficiency were 10 $e^-$ and 80%; atmospheric transmission = 75%; and optics transmission = 50%.

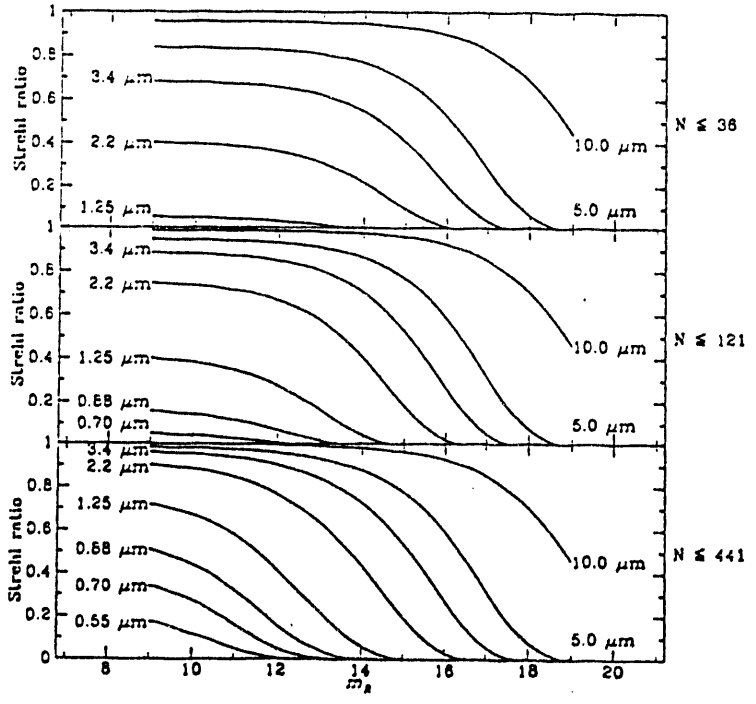


Figure 4. Optimized Strehl ratio for various observing wavelengths, as a function of reference star magnitude $m_R$. The bottom panel assumes a deformable mirror with 441 physical subapertures which can, under software control, be configured so as to mock up the behavior of a mirror with fewer subapertures. The middle and top panels correspond to deformable mirrors with ≤ 121 and ≤ 36 effective subapertures.

Let us examine Figure 4 in more detail.

At the *right* edge of each of the three panels, the reference stars are very faint and the adaptive optics systems are all starved for light. Hence the optimization routine has chosen to use the largest permissible subaperture area, in order to collect sufficient light from the very faint reference star to minimize the error due to poor signal-to-noise ratio. In fact, all three systems are using about 36 effective subapertures for magnitudes fainter than about 16. Hence the performance of the three systems is quite similar, for the faintest reference stars. There is little difference in the Strehl of the three systems as a function of observing wavelength, for dim reference stars.

By contrast at the *left* side of each panel, mirror fitting error is the largest wavefront error term when the reference star is bright, and the Strehl is limited by the inherent number of physical subapertures in each deformable mirror system (36, 121, or 441). Thus the system with the most possible subapertures ($N \leq 441$) has the largest Strehl ratio at short wavelengths. In particular, good Strehl at wavelengths shorter than 2.2 μm is only achieved for the $N \leq 121$ subaperture system, and good Strehl at wavelengths below 1.25 μm is only achieved for the $N \leq 441$ subaperture system.

The magnitude distribution of stars on the sky is a known quantity. While Figure 4 assumed that the reference star was within an isoplanatic angle of the object being observed, in reality a suitable reference star will be located at some mean distance from the object being imaged, generally larger than the isoplanatic angle. When one adds in the additional wavefront error due to anisoplanatism, one finds[7] that achieving Strehls > 0.2 with fractional sky coverage > 10% at $\lambda = 2.2$ μm requires using natural reference stars fainter than about $m_R = 14$. In this case, perusal of Figure 4 shows that *there is nothing to be gained* at 2.2 μm by building a natural guide star adaptive optics system with more than 121 physical subapertures, for a ten meter telescope. In fact, the optimum number of subapertures lies *between* N = 36 and 121. Thus based on statistical considerations alone, a near IR adaptive optics system using only natural reference stars need not have more than a few tens to a hundred subapertures. (The only reason to use more subapertures would be if one wanted to study the relatively few specific objects which happen to lie within 10 arc seconds or so of a bright star.)

These considerations have another consequence. For a ten meter telescope, in order to achieve fractional sky coverage > 10% the optimum observing wavelengths for natural guide star adaptive optics are longer than 2.2 μm, as one can see by mentally interpolating between the top two panels of Figure 4. However for wavelengths longer than 2.2 μm, thermal backgrounds become quite important. System design will be driven by the necessity to limit the overall emissivity. This can be done in several ways: using adaptive secondaries, cooled adaptive optics tables, and/or minimizing the number and emissivity of mirrors in the system. Such an adaptive optics system will probably end up looking quite different from one which was optimized for wavelengths between 0.8 and 2 μm.

However, the possibility of using *laser* reference stars strongly changes the conclusions one draws from Figure 4.

We shall show below that even modest-sized lasers at Mauna Kea can produce sodium laser guide stars having magnitudes between 8 and 10. Thus with a laser reference star, one will be operating on the *far left hand* side of Figure 4, where the Strehl in all the panels is being limited by deformable mirror fitting error. In this case there is a dramatic improvement in Strehl at wavelengths ≤ 2.2 μm, as one goes from 36 to 121 to 441 subapertures, and the performance at $\lambda = 1.25$ μm is quite acceptable even for the $N \leq 121$ subaperture system.

Thus if one is eventually going to have access to laser guide star, it is desirable to choose a deformable mirror having *well more than* 100 subapertures, for a ten meter telescope on Mauna Kea. The wavelength range of this system then emphasizes the region between 1 and 2.2 μm. Such a system would have the added advantage that it could perform at high Strehl ratios at wavelengths ≤ 2.2 μm for those astronomical objects which happen to lie near bright natural reference stars.

### 3.2 Segment vibration issues for the Keck Telescopes

The Keck Telescopes are unique in that their primary mirrors are constructed from an assembly of contiguous hexagonal segments. Each of these segments has a separate support structure, with all the support structures attached to a common frame

below. Such a design has the great advantage of light weight and favorable thermal characteristics, but it leads to the possibility that the segments can have vibrational modes independent of one another.

Measurements by Dekens et al.[3] using a fast-framing camera have shown that under some circumstances, the segments are seen to vibrate independently, with a peak in the power spectrum at about 29 Hz. Evidence to date suggests that this vibration is driven by specific heavy equipment associated with the Observatory. Thus once the source is better understood, it should be possible to greatly reduce the amplitude of the vibrations.

However, to the extent that residual vibrations remain, and depending on their RMS amplitudes, there could be strong implications for the overall architecture and the specific design of a Keck adaptive optics system. For example, one might need to compensate for vibration of the primary mirror segments by using a segmented adaptive mirror, either alone or in series with another deformable mirror in the adaptive optics train. The methodology for sensing the vibrations to be corrected by this mirror would need to be carefully studied, particularly if there is a significant component of piston in the residual vibration spectrum.

Because of these considerations, a vigorous effort will be needed to characterize the sources of these segment vibrations, and to understand the practical options for remedies.

## 4. LASER GUIDE STAR OPTIONS AND ISSUES

### 4.1 Available lasers

For a ten meter telescope, there is a strong preference for sodium-layer laser guide stars, because of the cone effect (focus anisoplanatism) which is much more adverse for Rayleigh guide stars.

Quantitative comparisons of the expected performance, cost, and deployment difficulties of alternative sodium lasers at Keck are just now getting under way. Thus far we have modeled three specific sodium guide star lasers, with $\lambda = 589$ nm:

1) A 2 watt CW ring dye laser available from Coherent, which emits in a single longitudinal mode. This dye laser is pumped by a 25 watt argon-ion laser. In the future it may be possible to double the output power using two 25 watt argon-ion pump lasers.

2) A 5 watt CW standing-wave dye laser built at LLNL, emitting in 2 or 3 modes, pumped by two 25-watt argon-ion lasers.

3) A pulsed dye laser (pulse length 150 nsec, pulse repetition frequency 30 kHz) developed in the Atomic Vapor Laser Isotope Separation Program at LLNL. This laser is phase-modulated to match the 2 GHz line width of the $D_2$ line in the atmospheric sodium layer, and is pumped via fiber optics by Nd:YAG lasers with intercavity frequency doublers. The pulsed dye laser operates in a master oscillator - power amplifier mode, and can produce average powers ranging from 30 watts to several hundred watts by adding power amplifiers (and their pump lasers) to the front of the chain.

### 4.2 Waste heat and thermal management issues

Because it has been shown that heat sources in the dome lead to degraded seeing, it is a policy of the Keck Observatory to limit thermal emission of sources within the dome to 100 watts or less. Sources emitting more than 100 watts are required to implement glycol cooling in order to dump their waste heat outside the dome.

This policy suggests the following considerations with regard to thermal management of waste heat from lasers. *Either:*

One should use inherently high-efficiency lasers, *and/or*

If there *are* low-efficiency components, one should place them outside the dome and then use optical fibers to bring light to the telescope, *and/or*

If the laser package *must* be placed in the dome, a cooling system needs to be engineered to carry the waste heat out of the dome in a cooling fluid.

These thermal management solutions take different forms for the three laser systems discussed above.

For the two CW dye lasers, most of the waste heat comes from the argon-ion pump lasers, which have efficiencies less than $5 \times 10^{-4}$. Two 25-watt argon-ion pump lasers produce more than 100 kW of waste heat. Because of their architecture, it would be difficult if not impossible to implement fiber-optic pumping of the CW dye lasers. Thus the argon-ion pump lasers must be located quite near the dye lasers which they are pumping. A location on the Nasmyth platform is plausible. In this case a cooling system would have to be implemented which will carry all but one part in $10^{-3}$ of the waste heat out of the dome. Since the Nasmyth platform is large and stable, one can think of building an insulated, liquid-cooled enclosure which could accomplish this level of heat rejection, although the cost of such an enclosure is at present not well established.

The pulsed dye laser is in a master oscillator - power amplifier configuration. As a result one can locate the Nd:YAG pump lasers outside the dome, bring in the green pump light through multi-mode optical fibers, and mount the dye laser directly on the telescope barrel. This is the architecture being used at the Lick Observatory[8] on the Shane 3 meter telescope. Within the dome itself the heat load for a 30 watt average power sodium laser is 50 watts of waste heat carried off in the dye lines to a heat exchanger outside the dome, and another 50 watts of waste heat carried away in glycol or other conventional cooling. Thus the thermal management issue appears easiest to solve for the pulsed dye laser, although it appears to be manageable at least in principle for the CW dye lasers as well.

### 4.3 Predicted adaptive optics system performance with laser guide stars

We have begun to model the sodium layer response due to each of the above lasers. The expected sodium-layer emission is then used in a systems-analysis model to predict the Strehl performance of laser guide star adaptive optics[9]. Figure 5 shows the first step in such models, computation of the expected equivalent magnitude of the laser guide star as a function of the average power of the laser system. For each of the curves in Figure 5 it is assumed that the spot size in the atmospheric sodium layer is a third of a meter, and that $r_0 = 20$ cm at a wavelength of 0.5 μm.

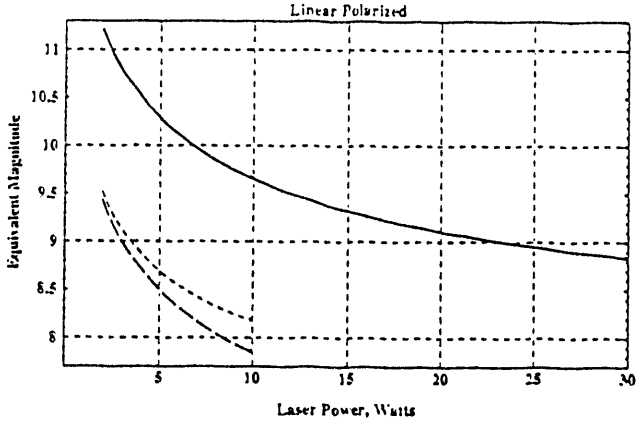


Figure 5. Equivalent magnitude of the sodium-layer laser guide star, as a function of the average power of the laser. Top curve is for a pulsed dye laser with 150 nsec pulse length and a 30 kHz pulse repetition rate. Light dashed curve (middle) is for a CW ring dye laser. Darker dashed curve (bottom) is for a CW standing-wave dye laser. Linear polarization of the laser light is assumed.

The pulsed dye laser is beginning to saturate the sodium layer even at a few watts of average power because of its much higher peak power. It thus creates a considerably dimmer guide star than the CW dye lasers of the same average power. The ring dye laser performs less well than the standing-wave laser because of its single-mode structure: the natural line profile of the atoms in the sodium layer is about 2 GHz wide, and thus the two or three modes of the standing wave laser can excite the sodium atoms more efficiently. We are currently repeating these atomic physics calculations using circular polarization, to assess the beneficial effects of optical pumping on the sodium layer return.

We have used the above guide star magnitude predictions in our system performance models, to estimate the system Strehl attainable with each of the above laser guide star systems. To the above three laser options we have added a fourth, consisting of the pulsed dye laser described above, with amplifiers added so as to produce 12 sodium guide star spots, each of 25 watts average power. This configuration can begin to address focus anisoplanatism for observing wavelengths shorter than 1 μm.

Figure 6 shows the Strehl expected as a function of laser wavelength, for four laser options. A deformable mirror having 273 subapertures is assumed. The bottom curve (light dashed line) is the CW ring dye laser with 2 watts of average power. The second curve (solid black line) is the pulsed dye laser with 30 watts of average power. The third curve from the bottom (large dark dashes) is the 5 watt standing-wave CW dye laser. The top curve (long and short dashes) is the 300 watt pulsed dye laser, distributed into 12 spots each with 25 watts average power.

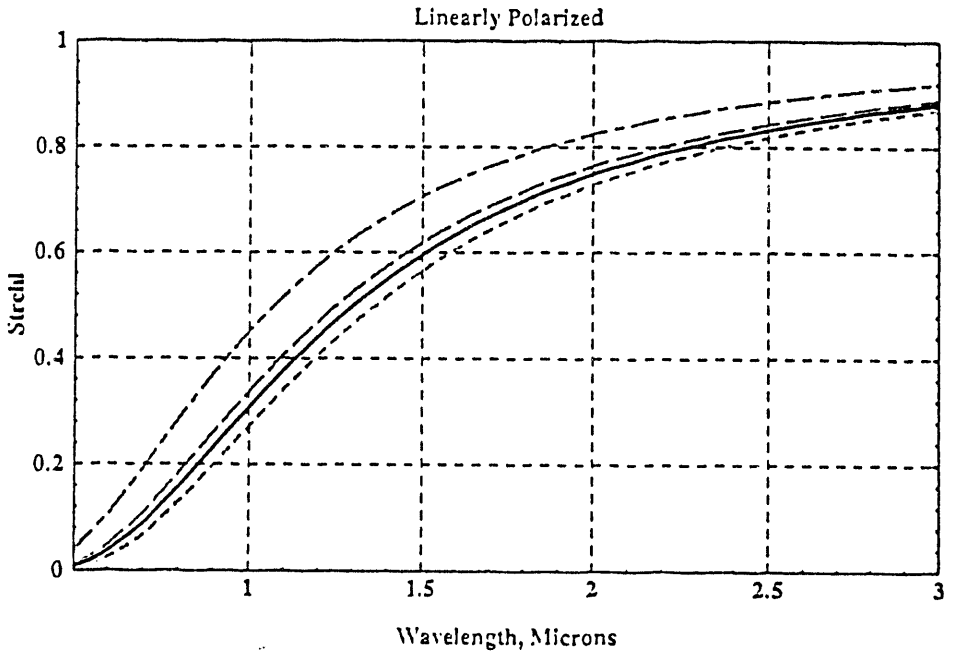


Figure 6. Predicted Strehl as a function of observing wavelength, for four different laser implementation options (see text above). The lasers have linear polarization; the adaptive optics system has 273 subapertures.

For wavelengths less than one micron, the Strehl is improved by a factor of 1.5 - 2 via use of multiple laser guide star spots. One would see an even more dramatic improvement from the use of multiple laser spots if the adaptive optics system had more than 273 subapertures, since at observing wavelengths less than a micron the system shown by the top curve in Figure 6 is being limited by the fitting error of the deformable mirror.

Finally, we can combine our optimization and sky coverage calculations with the above laser guide star performance curves, to obtain a comparison of the Strehl and sky coverage achievable using natural and laser guide stars. Figure 7 shows the predicted Strehl as a function of sky coverage fraction at observing wavelengths of $\lambda$ = 1.25, 2.2, and 3.4 $\mu$m for the 8 watt standing wave dye laser.

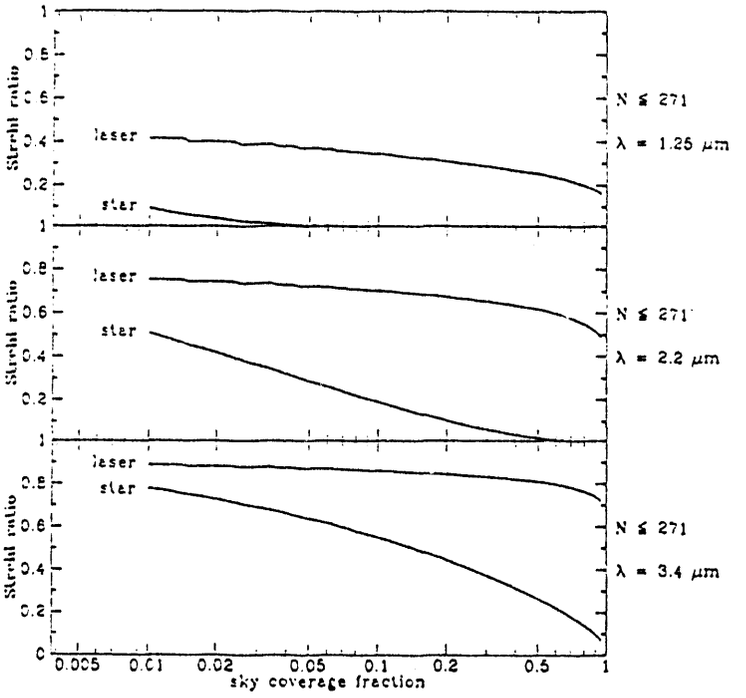


Figure 7. Optimized Strehl as a function of sky coverage fraction and observing wavelength. The adaptive optics system has N ≤ 271 subapertures, and the standing wave CW dye laser has 8 watts of power. The laser guide star calculation includes the requirement for an adequate tip-tilt reference star; the natural guide star calculation assumes that the wavefront reference is also used as a tip-tilt reference star.

One sees that the natural guide star adaptive optics system has good Strehl at low sky coverage fractions. But because of the lack of bright natural reference stars, the Strehl decreases strongly at sky coverage fractions larger than 10 - 20%. By contrast, the laser guide star system Strehl decreases much more slowly as one moves from low to high sky coverage fractions. In fact the predicted Strehl remains above 0.2 at all sky coverages even for an observing wavelength of 1.25 microns.

## 5. INSTRUMENTS FOR ADAPTIVE OPTICS

The true measure of an astronomical adaptive optics system is the quality and interest of the science which it enables. Thus the issues that are currently being debated in the Keck community are:

- What science can the Keck adaptive optics system do that will have the highest impact, and what instruments (new or existing) are needed to do this science?

- What competitive niche can science with a Keck adaptive optics system fill, in an era in which the Hubble Space Telescope (HST) and several adaptive optics systems on 8-meter ground-based-telescopes are fully functional?

Clearly one advantage of the Keck Telescopes compared with the Hubble Space Telescope arises from Keck's 10-meter aperture, which is four times larger than HST's. This means that in principle the diffraction-limited resolution is four times better at Keck, and that Keck's light-gathering power is sixteen times greater.

However, there are other factors which make Keck's comparative advantage over HST less evident for high angular resolution applications. First, adaptive optics at Keck is most likely to reach the diffraction limit for $\lambda > 0.8$ μm, at least in the forseeable future. HST will continue to be unmatched in the ultra-violet and blue parts of the spectrum. Second, HST's diffraction-limited field of view is quite large, compared to the field of view which will be available at the diffraction limit of Keck using adaptive optics. This suggests that HST will remain more powerful for multi-object work and for statistical cosmology, except for the faintest galaxies which only Keck's large collecting area can see in a reasonable exposure time.

Hence there are at least two niches for astronomical adaptive optics at Keck: single-object, high-resolution work (imaging and spectroscopy) in the red and infra-red, and studies of very faint objects over narrow patches of the sky. Indeed a likely mode of operation is that HST will discover interesting small-scale spatial structure in specific astronomical objects, and that Keck will be able to perform the needed follow-up observations with greater spatial resolution and with greater sensitivity. In addition, of course, HST does not yet have infra-red capabilities, and hence any contributions from infra-red adaptive optics at Keck will be unmatched by HST until the launch of NICMOS.

A second question of interest concerns how to design the Keck adaptive optics system so that it can make a unique science contribution compared with adaptive optics planned for other 8 meter telescopes. There is not yet a comprehensive response to this question. However, use of a modest (e.g. a few to twenty watts) laser guide star would give Keck the potential to achieve high Strehl ratios at observing wavelengths of 1 to 2.2 μm, with wavelengths as short as 0.8 μm accessible under favorable atmospheric conditions. This ability to access shorter observing wavelengths at the resolution of a ten meter telescope will enable Keck to contribute something genuinely new to the field of high-resolution astronomy.

### 5.1 High spatial resolution, narrow field of view applications

Near-infra-red detectors are about to appear with 1024 x 1024 pixel formats. If the diffraction limit of the 10 meter Keck Telescope is Nyquist-sampled in the near infra-red, even these larger detectors will yield only relatively narrow fields of view, on the order of 10 or 20 arc sec for wavelengths of 1 and 2 microns respectively. Hence although one competitive niche for the Keck Telescope is to take advantage of its very small diffraction limit, this comes at the price of a narrow field of view due to the present format limitations of infra-red arrays. The field-of-view limitation imposed by Nyquist-sampling of the Keck diffraction limit with 1024 x 1024 arrays is perhaps even more stringent than the field-of-view constraint which arises because of the isoplanatic angle.

Two near-infra-red instruments to take advantage of adaptive optics at the Keck Nasmyth platform are in the preliminary study phase at this time: a near-infra-red high-resolution imager, and a near-infra-red spectrograph with a narrow-slit mode for high spectral resolution. Since the design studies are still in progress, it is not yet appropriate to discuss these two instruments in detail.

### 5.2 Wider field of view applications with more moderate improvements in spatial resolution

An alternative approach is to attempt to provide a modest adaptive optics correction (e.g. a factor of a few improvement in enclosed energy width), but over a considerably wider field of view than with conventional adaptive optics (perhaps one or even two arc minutes). If this proves practical, it would be of great interest for multi-object work such as is needed in cosmology or in the study of star clusters and other densely populated fields. One might aim to be able to perform 10% accurate photometry over a field of an arc minute or so, with a well-understood point-spread function. At Mauna Kea, an improvement in the encircled energy by a factor of a few could bring the encircled energy radius down to values of a tenth arc second, a range which is of considerable interest for spectroscopy as well as for other applications.

Other authors have also emphasized the inherent interest of this type of adaptive optics capability; indeed the suggestion of multi-conjugate adaptive optics originated from a motivation similar to the one described above. These wider-field approaches need considerable study before being proven, and thus we regard this area as an important one for long-range investigation.

However in the short run, we would like to understand the issues well enough to design Keck adaptive optics hardware so that it will be able to accommodate wider field-of-view applications in the future, to the maximum extent possible.

## 6. SUMMARY

The Keck Observatory is beginning development of tip-tilt and adaptive optics systems, optimized for near infra-red observations. The initial tip-tilt system will serve a near infra-red camera, a 10 micron spectrograph, and a 10 micron camera at the forward Cassegrain focus of Keck I. The higher-order adaptive optics system will be located at a Nasmyth platform, and is intended to serve a near-infra-red imager and spectrograph which are now in the early design phase. A single-beacon sodium guide star will be implemented to increase the sky coverage available with the infra-red adaptive optics system, if permission to deploy such a laser on Mauna Kea can be obtained.

Calculations which optimize adaptive optics system performance using the existing distribution of natural stars predict that for a Strehl ratio greater than 0.2, a sky coverage fraction greater than 10% at 2.2 microns can be obtained using natural reference stars, and a sky coverage fraction greater than 80% at 1.25 microns can be obtained using a few-watt sodium laser guide star.

## 7. ACKNOWLEDGMENTS

At LLNL, this research was performed under the auspices of the U. S. Department of Energy, under contract number W-7405-ENG-48 to the Lawrence Livermore National Laboratory, through the LLNL Laboratory Directed Research and Development Program. Parts of this work were supported by the California Association for Research in Astronomy and by the LLNL Institute of Geophysics and Planetary Physics.

## 8. REFERENCES

1. P. L. Wizinowich, J. E. Nelson, T. S. Mast, and A. D. Gleckler, "W. M. Keck Observatory adaptive optics program," in this Conference Proceedings.

2. A. B. Meinel and M. P. Meinel, "Concept Definition: Keck Interferometric Imaging Array (KIIA)," NASA, 1992.

3. F. Dekens, D. Kirkman, G. A. Chanan, T. S. Mast, J. E. Nelson, P. L. Wizinowich, and G. Illingworth, "High-speed seeing measurements at the W. M. Keck Observatory," in this Conference Proceedings.

4. G. A. Tyler, "The impact of centroid measurement upon pointing accuracy," Report no. TR-634 (the Optical Sciences Company, Placentia, CA) 1985.

5. S. S. Olivier, C. E. Max, D. T. Gavel, and J. M. Brase, "Tip-tilt compensation: resolution limits for ground-based telescopes using laser guide star adaptive optics,", *Astrophys. J.* , Vol. 407, pp. 428-439, 1993.

6. S. S. Olivier and D. T. Gavel, "Tip-tilt compensation for astronomical imaging," *J. O. S. A.* ,Vol. A11, pp. 368-378, 1994.

7. S. S. Olivier, "Optimized performance of natural reference star adaptive optics systems,", submitted to *Astrophys. J.*, 1994.

8. H. W. Friedman, T. Kuklo, J. N. Wong, R. H. Page, and G. R. Thompson, "Design of a fieldable laser system for a sodium guide star,", in this Conference Proceedings.

9. D. T. Gavel and S. S. Olivier, "Simulation and analysis of laser guide star adaptive optics systems for the 8- to 10-meter-class telescopes," in this Conference Proceedings.

DATE
FILMED
5/19/94
END